JACS
JOURNAL OF THE AMERICAN CHEMICAL SOCIETY
Communication
pubs.acs.org/JACS

Rapid Measurement of Pseudocontact Shifts in Metalloproteins by Proton-Detected Solid-State NMR Spectroscopy

Michael J. Knight,[†] Isabella C. Felli,[‡] Roberta Pierattelli,*[,‡] Ivano Bertini,[‡,§] Lyndon Emsley,[†] Torsten Herrmann,[†] and Guido Pintacuda*[,†]

[†]Centre de RMN à Très Hauts Champs, UMR 5280 CNRS/ENS Lyon/UCB Lyon 1, Université de Lyon, 5 rue de la Doua, 69100 Villeurbanne, France

[‡]Department of Chemistry "Ugo Schiff" and Magnetic Resonance Center (CERM), University of Florence, via Luigi Sacconi 6, 50019 Sesto Fiorentino, Italy

Supporting Information

ABSTRACT: Pseudocontact shifts (PCSs) arise in paramagnetic systems in which the susceptibility tensor is anisotropic. PCSs depend upon the distance from the paramagnetic center and the position relative to the susceptibility tensor, and they can be used as structural restraints in protein structure determination. We show that the use of ^{1}H-detected solid-state correlations provides facile and rapid detection and assignment of site-specific PCSs, including resolved ^{1}H PCSs, in a large metalloprotein, Co^{2+}-substituted superoxide dismutase (Co^{2+}-SOD). With only 3 mg of sample and a small set of experiments, several hundred PCSs were measured and assigned, and these PCSs were subsequently used in combination with ^{1}H–^{1}H distance and dihedral angle restraints to determine the protein backbone geometry with a precision paralleling those of state-of-the-art liquid-state determinations of diamagnetic proteins, including a well-defined active site.

Metal ions play an important role in a large variety of biochemical and cellular processes, and most of them are paramagnetic because of the presence of unpaired electrons.[1,2] Paramagnetic effects have long been used and today play a central role in NMR structural determinations of metalloproteins[3−5] and biomolecules covalently modified with a spin label.[6,7] Paramagnetic effects can manifest themselves as either shifts (contact or "pseudocontact" shifts) or paramagnetic relaxation enhancements (PREs), depending on the character of the metal center.

Pseudocontact shifts (PCSs) are the consequence of an anisotropic susceptibility tensor (χ).[8] These effects act over very long distances and carry a well-defined geometrical dependence on the nuclear position with respect to the principal axes of χ anchored on the paramagnetic center. PCSs are straightforward to evaluate experimentally, simply as the difference between the chemical shifts of the paramagnetic species and an isostructural diamagnetic analogue. PCSs are easy to model from the χ anisotropy and its orientation, and they are routinely used in solution NMR spectroscopy together with other data to refine structures,[5,9] to investigate protein−protein interactions,[10,11] and to monitor dynamics.[12−14] However, these effects are always associated with Curie relaxation enhancements, which are a result of the molecular tumbling in solution.[15] They are therefore of particular interest when a paramagnetic sample is studied in the solid state, in which the Curie broadening is absent.[16,17]

In recent years, solid-state NMR (ssNMR) spectroscopy has significantly progressed to become a powerful tool for the structural and dynamical characterization of a variety of biological materials ranging from microcrystalline samples to fibrils and membrane-associated systems,[18,19] but in only a few cases has its potential been realized for paramagnetic metalloproteins.[17,20−22] This is a result of the fact that despite the absence of Curie broadening, a number of competing effects make the detection of signals close to a paramagnetic center difficult in the solid state. A key improvement in this regard has been provided by the use of very fast (>30 kHz) magic-angle-spinning (MAS) probes.[23,24] This has allowed efficient detection of previously unobservable nuclei in highly paramagnetic materials, disclosing a rich amount of information that can be directly linked to the electronic and molecular structure. These techniques have been used on highly paramagnetic proteins, significantly reducing the blind sphere close to the metal center with respect to solution studies.[17,25]

Despite these few proof-of-principle papers, however, these approaches have not become very popular because they require very laborious studies and are far from being routine.[21,26,27] General limits include the sensitivity and resolution offered by traditional detection and assignment methods. This problem can be partially alleviated by the enhanced longitudinal relaxation caused by the paramagnetic center, which can be exploited for fast recycling[28] and condensed data collection approaches relying on ^{13}C detection.[29] More recently, we have shown that in combination with perdeuteration, ultrafast MAS enables ^{1}H detection and accelerated acquisition of resolved "fingerprint" spectra of proteins,[30] from which a variety of site-specific structural and dynamical parameters can be rapidly measured.[31]

Here we show that the use of ^{1}H-detected solid-state correlations provides facile and rapid detection and assignment of site-specific PCSs, including resolved ^{1}H PCSs, in a large metalloprotein. We used a perdeuterated sample of the

Received: July 12, 2012
Published: August 23, 2012

dx.doi.org/10.1021/ja306813j | J. Am. Chem. Soc. 2012, 134, 14730−14733

metalloenzyme superoxide dismutase (SOD; 2 × 16 kDa),[32] which has two high-affinity binding sites for metal cations. The metalation state can be controlled experimentally to obtain samples having the desired paramagnetic effects with minimal structural perturbation. In this study, we employed a paramagnetic sample and its diamagnetic analogue in which one site was empty and a (paramagnetic) Co^{2+} or a (diamagnetic) Zn^{2+} ion, respectively, occupied the second site (as occurs in the most common physiological form, Cu^{2+},Zn^{2+}-SOD). Several hundred PCSs were measured and assigned by comparing the shifts of Co^{2+}-SOD and Zn^{2+}-SOD, and these PCSs were subsequently used in combination with $^1H-^1H$ distance and dihedral angle restraints to determine the protein backbone geometry with a precision paralleling that of state-of-the-art liquid-state determinations of diamagnetic proteins, including a well-defined active site.

In Figure 1a we show ^1H-detected cross-polarization (CP)−heteronuclear single-quantum correlation (HSQC) spectra of Zn^{2+}-SOD and Co^{2+}-SOD. The fast electron relaxation of Co^{2+} does not cause large PREs (the electronic relaxation time is in the range 1−10 ps[33]), and the ^{15}N, ^{13}C, and ^1H coherence lifetimes are long enough to facilitate the acquisition of well-resolved multidimensional spectra. Perdeuteration is extremely powerful toward this aim, as it significantly weakens the $^1H-^1H$ dipolar coupling bath. The resolution limits of the CP−HSQC spectrum, which are inhomogeneous in origin, can thus be overcome by recording three-dimensional (3D) correlations. They can be performed very rapidly using ^1H detection without any significant loss of signal. We used 3D (H)CONH and (H)CANH experiments[30] to obtain resolved resonances for Co^{2+}-SOD. Planes from the (H)CONH experiment are shown in Figure 1c−g. Full experimental details are given in the Supporting Information (SI). Notably, very few of the spins close to the metal escaped detection in these experiments. For example, in both the (H)CONH and (H)CANH spectra we were able to observe resonances for His63, whose amide proton in the X-ray structure of the homologous Cu^{2+},Zn^{2+}-SOD is only 5.2 Å from the Zn^{2+} ion, which here is replaced by Co^{2+}.

With these spectra in hand, along with the availability of reference shifts and an approximate structure model for the diamagnetic analogue, the assignment of PCSs and their use as structural restraints was implemented as an iterative procedure.

The assignment was particularly straightforward, exploiting the systematic change in chemical shifts along "diagonal" lines in the spectra characteristic of PCS effects, as illustrated in Figure 1c. To assign Co^{2+}-SOD resonances, we used the existing Zn^{2+}-SOD assignments[30] and then assigned those Co^{2+}-SOD resonances that were easily identifiable from the comparison of spectra. An approximate χ tensor was then fitted to the PCSs determined from these assignments on the basis of the ssNMR fold of SOD (such as obtained from ^1H,^1H distance restraints in Cu^{1+},Zn^{2+}-SOD), and all other resonances were predicted. More assignments could then be made, and the process was repeated until all of the peaks visible in the 3D spectra were assigned and a consistent χ tensor was obtained. This and the spatial dependence of the PCSs are illustrated in Figure 1b,c. This method also required that the Co position be determined from PCSs, so that eight parameters (the two χ tensor anisotropies, the three angles defining its orientation, and the three metal coordinates) had to be fitted for a full determination of the χ tensor. An approximate starting position for the Co ion was obtained from the resonances broadened by the Co PRE.

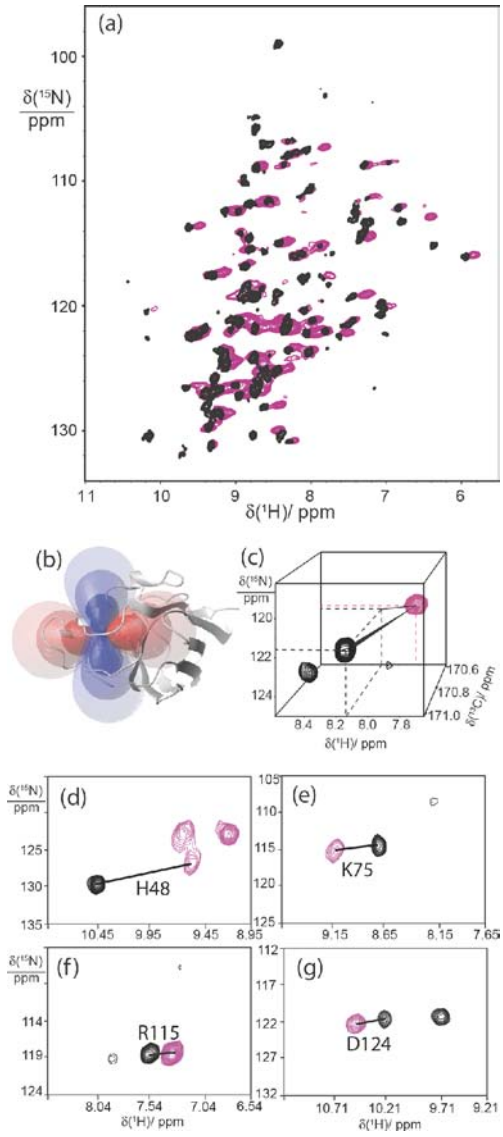

Figure 1. (a) Solid-state ^1H,^{15}N correlation spectra (CP−HSQC) of Co^{2+}-SOD (magenta) and Zn^{2+}-SOD (black) recorded at 800 MHz using 60 kHz MAS [32 scans, 0.7 s interscan delay, 256 t_1 increments, $t_1^{max}(^{15}N)$ = 38 ms, $t_2^{max}(^1H)$ = 15 ms, total time = 2 h]. (b) χ tensor for Co^{2+}-SOD in the solid state, represented as a set of PCS isosurfaces. Blue surfaces represent positive PCSs and red surfaces negative PCSs. The innermost, middle, and outermost surfaces represent PCSs of 1, 0.25, 0.1 ppm, respectively. (c) Identification of a PCS in a 3D (H)CONH spectrum [80 scans, 0.3 s interscan delay, 80 $t_1(^{15}N)$ increments, $t_1^{max}(^{15}N)$ = 4 ms, 92 $t_1(^{13}C)$ increments, $t_1^{max}(^{13}C)$ = 4.6 ms, $t_2^{max}(^1H)$ = 15 ms, total time = 45 h] with the same color scheme as in (a) along a characteristic diagonal line. (d−g) Examples of PCS assignments from the (H)CONH spectra, where the planes are overlaid in such a way that the labeled peaks are at their respective maxima in the ^{13}C dimension. The solid black lines indicate the PCSs. More experimental details can be found in the SI.

A χ tensor was obtained for which the axial and rhombic components were $(1.03 \pm 0.03) \times 10^{-32}$ and $(0.91 \pm 0.02) \times 10^{-32}$ m^3, respectively, and a total of 445 PCSs (111 ^1H, 223 ^{13}C, and 111 ^{15}N) could be assigned in this way. To take into account the fact that some regions of the structures were better defined than others, when a χ tensor was fitted, the errors in the PCSs were weighted by the bundle root-mean-square deviations (rmsd's) for the residues from which the PCSs

dx.doi.org/10.1021/ja306813j | J. Am. Chem. Soc. 2012, 134, 14730−14733

originated. By such means, ill-defined regions of the starting ssNMR structure bundles were given less influence in the fitting procedure than well-defined regions. Overall, this process was effectively guided by ^{1}H, ^{13}CO, and $^{13}C\alpha$ shifts, while the evaluation of ^{15}N PCS was found to be less accurate, as often is the case in previous literature.[34,35]

For the structural calculation, PCSs were subsequently used in combination with $^{1}H-^{1}H$ distance restraints (totaling 297 $^{1}H-^{1}H$ pairs), dihedral angle restraints, and ambiguous hydrogen bond restraints in the program Cyana.[36] The use of these paramagnetic restraints significantly reduced the backbone rmsd of the final ensemble from 2.90 to 1.71 Å. In particular, the definition of the backbone geometry was extremely well defined in the proximity of the Co^{2+} binding site. The resulting structure bundles are shown in Figure 2a–d.

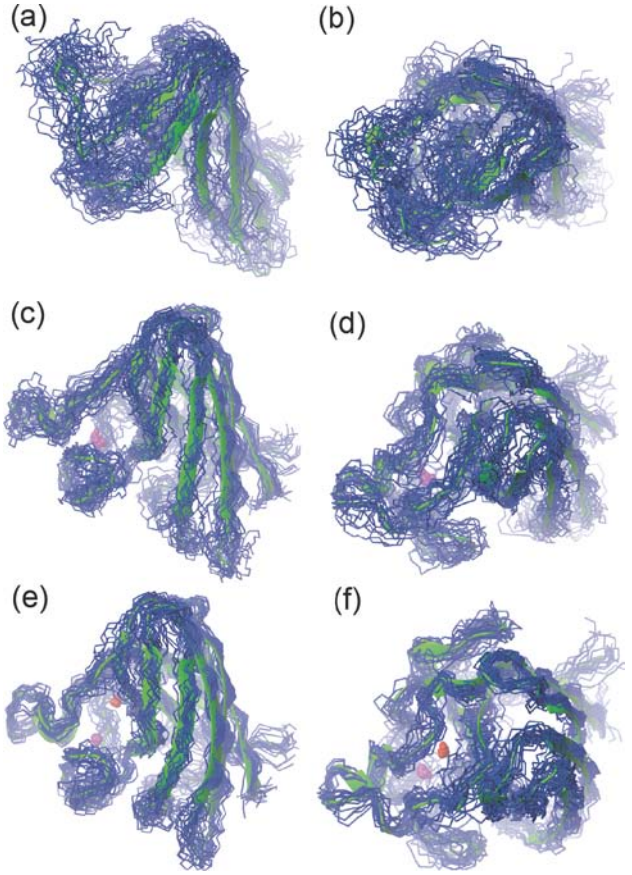

Figure 2. ssNMR structure bundles for SOD with different views and different types of paramagnetic restraints: (a, b) with no paramagnetic restraints; (c, d) with PCSs, with the χ tensor being fitted using the structure shown in (a, b); (e, f) with both PCSs and PREs. Magenta is used for the Co^{2+} ion and red for the Cu^{2+} ion, and the green ribbon diagram in each case is the mean NMR structure. The atomic coordinates of structures (c, d) and (e, f) have been deposited in the Protein Data Bank.

The excellent correlation between the experimental and back-calculated PCSs shown in Figure 3a indicates that in a protein of this size we can legitimately treat the PCSs as purely intramolecular.

The quality of the NMR structure was further improved when PCSs were used in combination with PRE-derived distance restraints. To illustrate this point, PRE-derived distance restraints as measured for Cu^{2+}-SOD[31] were

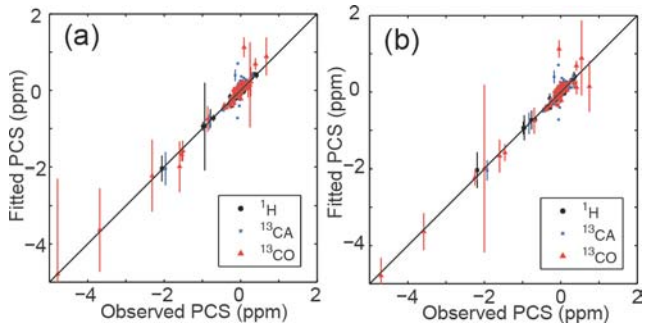

Figure 3. Correlations between the measured PCSs and the values back-calculated using the final structural ensemble (a) with diamagnetic restraints and PCSs and (b) when PRE-derived restraints were used. Perfect agreement is indicated by the diagonal black lines.

implemented (Figure 2e,f). The incorporation of these additional data did not alter the χ tensor fitting procedure (Figure 3; also see the SI). The backbone rmsd dropped to 1.39 Å, and the protein backbone was determined with very good precision at both metal sites, allowing the entire active site to be modeled.

It is interesting to note here that the χ tensor magnitudes and thus the PCSs determined for Co^{2+}-SOD were around an order of magnitude smaller than those observed for microcrystalline Co^{2+}-substituted matrix metalloprotease 12 (Co-MMP12).[21] The low PCSs were in some ways beneficial here, since the complicating neighbor effects did not have to be taken into consideration and each PCS was almost entirely the result of the intramolecular Co^{2+} ion. This was validated by the fact that we also fitted a χ tensor to the PCS data using a SOD dimer in the crystal structure 1SOS (see the SI). The same χ tensor (within the experimental error) could be obtained without taking into account the fact that SOD is dimeric or if additional neighboring molecules were modeled according to published crystal structures. We note that if this were not the case, methods to delineate the contributions of inter- and intramolecular effects do exist.[21]

In conclusion, we have demonstrated that a proton-detected strategy for determining PCSs in a microcrystalline metalloprotein is straightforward and can significantly improve a structure calculated with ssNMR spectroscopy. The approaches presented here can be extended to other metalloproteins in which the metalation state can be made subject to experimental control or to which a paramagnetic tag can be attached. In addition, we have shown that an ssNMR structure bundle serves as an adequate model for fitting PCSs and obtaining χ tensor parameters for subsequent refinement. This will be important in systems for which no existing model is available, such as many membrane proteins or fibrils.

■ ASSOCIATED CONTENT

Supporting Information

Sample preparation and experimental details, χ tensor isosurface found using PRE and PCS restraints from ssNMR models, χ tensor obtained using X-ray crystallographic models of monomeric and dimeric SOD, and tables of measured solid-state PCSs. This material is available free of charge via the Internet at http://pubs.acs.org.

dx.doi.org/10.1021/ja306813j | J. Am. Chem. Soc. 2012, 134, 14730–14733

AUTHOR INFORMATION

Corresponding Author

pierattelli@cerm.unifi.it; guido.pintacuda@ens-lyon.fr

Notes

The authors declare no competing financial interest.
[§]Deceased July 7, 2012.

ACKNOWLEDGMENTS

This work is dedicated to the memory of Professor Ivano Bertini.

We acknowledge support from the Agence Nationale de la Recherche (ANR 08-BLAN-0035-01 and 10-BLAN-713-01), Ente Cassa di Risparmio di Firenze, Egide (Programme Galiée 22397RJ and 26000XF), the Università Italo Francese (Programma Galileo 26000XF), and Joint Research Activity and Access to Research Infrastructures in the Seventh Framework Program of the EC (EAST-NMR 228461 and BioNMR 261863).

REFERENCES

(1) *Handbook on Metalloproteins*; Bertini, I., Sigel, A., Sigel, H., Eds.; Marcel Dekker: New York, 2001.
(2) *Handbook of Metalloproteins*; Messerschmidt, A., Huber, R., Wieghardt, K.;, Poulos, T., Eds.; Wiley: Chichester, U.K., 2001.
(3) Banci, L.; Bertini, I.; Eltis, L. D.; Felli, I. C.; Kastrau, D. H.; Luchinat, C.; Piccioli, M.; Pierattelli, R.; Smith, M. *Eur. J. Biochem.* **1994**, *225*, 715−725.
(4) Bertini, I.; Luchinat, C.; Parigi, G.; Pierattelli, R. *ChemBioChem* **2005**, *6*, 1536−1549.
(5) Otting, G. *Annu. Rev. Biophys.* **2010**, *39*, 387−405.
(6) Otting, G. *J. Biomol. NMR* **2008**, *42*, 1−9.
(7) Keizers, P. M.; Ubbink, M. *Prog. NMR Spectrosc.* **2011**, *58*, 88−96.
(8) Bertini, L.; Luchinat, C.; Parigi, G. *Prog. NMR Spectrosc.* **2002**, *40*, 249−273.
(9) Arnesano, F.; Banci, L.; Piccioli, M. *Q. Rev. Biophys.* **2005**, *38*, 167−219.
(10) Pintacuda, G.; John, M.; Su, X. C.; Otting, G. *Acc. Chem. Res.* **2007**, *40*, 206−212.
(11) Clore, G. M.; Iwahara, J. *Chem. Rev.* **2009**, *109*, 4108−4139.
(12) Bertini, I.; Bianco, C. D.; Gelis, I.; Katsaros, N.; Luchinat, C.; Parigi, G.; Peana, M.; Provenzani, A.; Zoroddu, M. A. *Proc. Natl. Acad. Sci. U.S.A.* **2004**, *101*, 6841−6846.
(13) Wang, X.; Srisailam, S.; Yee, A. A.; Lemak, A.; Arrowsmith, C.; Prestegard, J. H.; Tian, F. *J. Biomol. NMR* **2007**, *39*, 53−61.
(14) Eichmüller, C.; Sckrynnikov, N. R. *J. Biomol. NMR* **2007**, *37*, 79−95.
(15) Vega, A. J.; Fiat, D. *Mol. Phys.* **1976**, *31*, 347−355.
(16) Kervern, G.; Steuernagel, S.; Engelke, F.; Pintacuda, G.; Emsley, L. *J. Am. Chem. Soc.* **2007**, *129*, 14118−14119.
(17) Pintacuda, G.; Giraud, N.; Pierattelli, R.; Böckmann, A.; Bertini, I.; Emsley, L. *Angew. Chem., Int. Ed.* **2007**, *46*, 1079−1082.
(18) McDermott, A. E. *Annu. Rev. Biophys* **2009**, *38*, 385−403.
(19) *NMR of Biomolecules: Towards Mechanistic Systems Biology*; Bertini, I., McGreevy, K. S., Parigi, G., Eds.; Wiley-VCH: Weinheim, Germany, 2012.
(20) Jovanovic, T.; Farid, R.; Friesner, R. A.; McDermott, A. E. *J. Am. Chem. Soc.* **2005**, *127*, 13548−13552.
(21) Balayssac, S.; Bertini, I.; Bhaumik, A.; Lelli, M.; Luchinat, C. *Proc. Natl. Acad. Sci. U.S.A.* **2008**, *105*, 17284−17289.
(22) Turano, P.; Lalli, D.; Felli, I. C.; Theil, E. C.; Bertini, I. *Proc. Natl. Acad. Sci. U.S.A.* **2010**, *107*, 545−550.
(23) Ishii, Y.; Wickramasinghe, N. P.; Chimon, S. *J. Am. Chem. Soc.* **2003**, *125*, 3438−3439.
(24) Kervern, G.; Pintacuda, G.; Zhang, Y.; Oldfield, E.; Roukoss, C.; Kuntz, E.; Herdtweck, E.; Basset, J. M.; Cadars, S.; Lesage, A.; Coperet, C.; Emsley, L. *J. Am. Chem. Soc.* **2006**, *128*, 13545−13552.
(25) Bertini, I.; Emsley, L.; Lelli, M.; Luchinat, C.; Mao, J.; Pintacuda, G. *J. Am. Chem. Soc.* **2010**, *132*, 5558−5559.
(26) Balayssac, S.; Bertini, I.; Lelli, M.; Luchinat, C.; Maletta, M. *J. Am. Chem. Soc.* **2007**, *129*, 2218−2219.
(27) Bertini, I.; Bhaumik, A.; De Paëpe, G.; Griffin, R. G.; Lelli, M.; Lewandowski, J. R.; Luchinat, C. *J. Am. Chem. Soc.* **2010**, *132*, 1032−1040.
(28) Wickramasinghe, N. P.; Parthasarathy, S.; Jones, C. R.; Bhardwaj, C.; Long, F.; Kotecha, M.; Mehboob, S.; Fung, L. W.; Past, J.; Samoson, A.; Ishii, Y. *Nat. Methods* **2009**, *6*, 215−218.
(29) Nadaud, P. S.; Helmus, J. J.; Sengupta, I.; Jaroniec, C. P. *J. Am. Chem. Soc.* **2010**, *132*, 9561−9563.
(30) Knight, M. J.; Webber, A. L.; Pell, A. J.; Guerry, P.; Barbet-Massin, E.; Bertini, I.; Felli, I. C.; Gonnelli, L.; Pierattelli, R.; Emsley, L.; Lesage, A.; Herrmann, T.; Pintacuda, G. *Angew. Chem., Int. Ed.* **2011**, *50*, 11697−11701.
(31) Knight, M. J.; Pell, A. J.; Bertini, I.; Felli, I. C.; Gonnelli, L.; Pierattelli, R.; Herrmann, T.; Emsley, L.; Pintacuda, G. *Proc. Natl. Acad. Sci. U.S.A.* **2012**, *109*, 11095−11100.
(32) McCord, J. M.; Fridovich, I. *J. Biol. Chem.* **1969**, *244*, 6049−6055.
(33) Bertini, I.; Luchinat, C.; Parigi, G. *Solution NMR of Paramagnetic Molecules: Applications to Metallobiomolecules and Models*; Elsevier: Amsterdam, 2001; Vol. 2.
(34) Bertini, I.; Luchinat, C.; Turano, P. *J. Biol. Inorg. Chem.* **2000**, *5*, 761−764.
(35) Jensen, M. R.; Hansen, D. F.; Ayna, U.; Dagil, R.; Hass, M. A. S.; Christensen, H. E. M.; Led, J. J. *Magn. Reson. Chem.* **2006**, *44*, 294−301.
(36) Herrmann, T.; Guntert, P.; Wüthrich, K. *J. Biomol. NMR* **2002**, *24*, 171−189.